THERMAL EFFECTS ON THE COMPRESSIVE BEHAVIOR OF IM7/PETI5 LAMINATES

Sandra Polesky Walker
NASA, Langley Research Center, MS 396, Hampton, VA 23681
(757)864-5434 , fax: (757)864-7943, email: s.p.walker@larc.nasa.gov

Presented at the
Fourteenth International Conference on Composite Materials
July 14-18, 2003
San Diego, CA

THERMAL EFFECTS ON THE COMPRESSIVE BEHAVIOR OF IM7/PETI5 LAMINATES

Sandra Polesky Walker
NASA, Langley Research Center, MS 396, Hampton, VA 23681
(757)864-5434 , fax: (757)864-7943, email: s.p.walker@larc.nasa.gov

ABSTRACT

The effect of changing operating temperature on the compressive response of IM7/PETI5 composite laminates is investigated within this paper. The three temperatures evaluated for this study were –129°C, 21°C, and 177°C, a spectrum from cryogenic to an elevated operating temperature. Laminate compressive strength property testing was conducted using the Wyoming Combined Load Compression fixture to generate strength data at the three operating temperatures of interest for several lay-ups. A three-dimensional finite element analysis model of a $[90/0]_{8s}$ composite laminate subject to compressive loading is developed. The model is used to study the key attributes of the laminate that significantly influence the state of stress in the laminate. Both the resin rich layer located between lamina and the thermal residual stresses present in the laminate due to curing are included in the analysis model. For the laminate modeled, the effect of modeling temperature dependent material properties was determined to be insignificant for the operating temperatures studied. Simply using the material properties measured at the operating temperature of interest was sufficient for predicting stresses accurately in a linear analysis for the current problem. The three-dimensional analysis results revealed that the application of an applied compressive axial load in the 0-degree direction decreased the interlaminar stresses present in the laminate initially due to curing. Therefore, failure was concluded not be attributable to the interlaminar stresses in the composite laminate being studied when a compressive load is applied. The magnitude of the measured laminate compressive strength change with a change in temperature is concluded to be dominated by the change in the lamina compressive axial strength with a change in temperature.

Keywords: composite laminates, environmental effects, compression strength, thermal, cure stresses, residual stresses

INTRODUCTION

Advanced technology vehicles require composite structural components to operate at temperature extremes while remaining lightweight. For a Mach 2.4 flight condition, temperatures up to 177°C have been predicted on the wing surface of a high-speed civil transport concept [1]. At the other end of the spectrum, a composite intertank concept, where due to proximity to a cryogenic tank in a launch vehicle, would expose the intertank to temperatures down to –129°C [2]. A polymer matrix material system, IM7/PETI5, has been developed for advanced vehicle applications [3]. The IM7/PETI5 material system was chosen here for study due to its unique characteristics and potential for use under high compressive loads at varying temperature conditions.

Prior studies of graphite/epoxy laminates have shown that significant residual stresses can develop in a laminate due to curing [4, 5, 6]. The IM7/PETI5 laminates have a glass transition temperature, T_g, of 238°C which is much higher than the T_g of 177°C for graphite/epoxy. Consequently, IM7/PETI5 laminates may develop more significant residual stresses than observed in prior studies and will consequently be investigated here. For this study, the extent to which the residual cure stresses vary with operating temperature and influence the change in strength of the laminate with temperature is of key interest.

Where the strength of polymer matrix composites are well known to be sensitive to operating temperatures, the objective of this study was to gain a more fundamental understanding on the behavior of the IM7/PETI5 material system at varying operating temperatures. Specifically, the mechanism for failure under compressive loading was studied. The scope of this study includes both laminate compression testing to generate strength data at the operating temperatures of interest, and a detailed three-dimensional finite element analysis study. The analyses were conducted on a $[90/0]_{8s}$ laminate to determine the key attributes and laminate detail required to predict stresses accurately. Residual thermal stresses due to curing were included for evaluation and the resin layers located between lamina in the laminate were also included in the detailed three-dimensional analysis model. Analysis results were used in an evaluation of the stress components associated with failure of the laminates.

MATERIAL PROPERTIES AND CHARACTERISTICS

The properties and characteristics of the IM7/PETI5 material system utilized in the analysis study are presented in this section. The measured IM7/PETI5 temperature-dependent orthotropic lamina material properties are given in Table 1, which were taken from Reference [7].

Table 1. IM7/PET5 Lamina Material Properties

Material Property	Test Temperature			
	-129°C	21°C	177°C	257 °C
E_{11C}(GPa)	141.	141.	141.	141.
F_{11C} (MPa)	1641.	1551.	1276.	
E_{11T}(GPa)	151.	151.	158.	178.
F_{11T} (MPa)	2317.	2117.	2117.	
E_{22C} (GPa)	13.8	15.2	10.3	8.3
F_{22C}(MPa)	324.	255.	185.	
E_{22T} (GPa)	11.	9.65	6.69	4.14
F_{22T} (MPa)	45.5	62.	50.3	
G_{12}(GPa)	7.17	6.34	4.76	4.27
F_{12}(MPa)	123.	100.	45.5	
ν_{12}	.34	.34	.33	
ν_{23}	.4	.64	.52	
F_{13}(MPa) - ILSS	147.	119.	82.7	
F_{33}(MPa) - ILNS	35.9	31.	18.6	
α_1(μm/m /C)	-.43	-.16	1.6	
α_2(μm/m/C)	18.1	27.9	30.1	

Since compression was the primary loading condition studied, compressive stresses were assumed to dominate and for simplicity only the compressive moduli, E_{11c} and E_{22c}, are used in the analysis models. The additional out-of-plane properties needed for a three-dimensional characterization of the composite are assumed related to the in-plane properties as follows,

$$E_{33} = E_{22} \tag{1}$$

$$G_{31} = G_{12} \tag{2}$$

$$G_{23} = \frac{E_{22}}{2(1+\nu_{23})} \tag{3}$$

$$\nu_{31} = \nu_{21} = \frac{E_{22}}{E_{11}}\nu_{12} \qquad \text{where} \quad \nu_{13} = \nu_{12} \tag{4}$$

$$\alpha_3 = \alpha_2 \tag{5}$$

and are determined from the properties previously given in Table 1.

For predicting residual cure stresses in the IM7/PETI5 laminates, the T_g is assumed to be the stress free temperature (SFT) below which thermal curing stresses develop in the laminates. The choice of the T_g as the SFT is in accord with previous investigations on curing stresses in graphite/epoxy laminates [8, 9]. Therefore, the measured $T_g = 238^oC$ is assumed to be the SFT in the current investigation for the IM7/PETI5 material.

Inclusion of resin-rich layers between plies, through the thickness of the laminate, was previously reported to affect significantly the interlaminar stresses [10]. A micrograph showing a 500 times magnification through the thickness of one of the $[90/0]_{8s}$ IM7/PETI5 laminate specimens is displayed in Figure 1. The micrograph shows an entire 90 degree layer located between two 0 degree plies. As can be observed in the micrograph, indeed there are resin-rich layers between lamina in the current IM7/PETI5 laminates, which will be incorporated into analysis models for predicting interlaminar stresses. This resin-rich layer was also observed in the unidirectional laminates, which should be accounted for in evaluations on material behavior. The properties of the resin-rich layer between lamina are assumed to resemble the 2-direction properties of the IM7/PETI5 material, which are dominated by the PETI5 resin properties. The PETI5 resin layer is hence assumed to be an isotropic material with the following two independent properties,

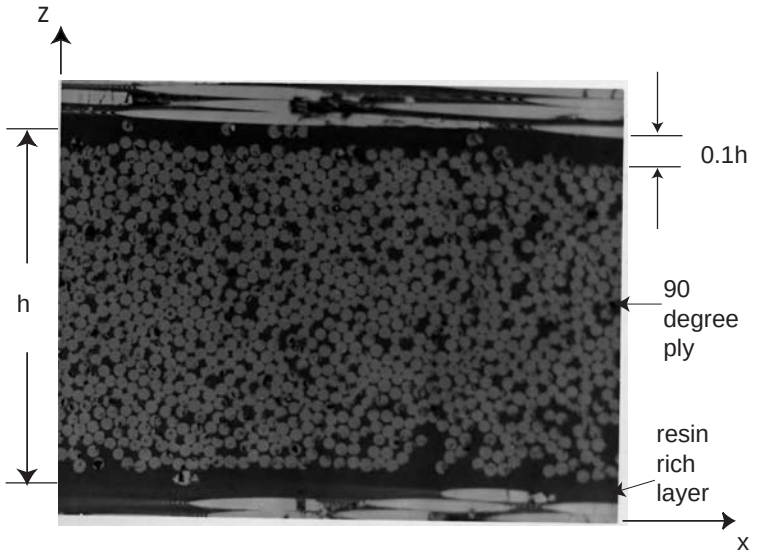

Figure 1. Micrograph showing a 500 times magnification through the thickness of a $[90/0]_{8s}$ IM7/PETI5 laminate.

$$E_r = E_{22} \tag{6}$$

$$\nu_r = 0.4 \tag{7}$$

LAMINATE COMPRESSION PROPERTY TESTING

To observe the effect of temperature change on compressive strength for IM7/PETI5 laminates, coupon specimens of several lay-ups were tested. Several lay-ups were chosen to evaluate strength changes for differing laminate constructions and to determine if any anomalies existed. The Combined Load Compression (CLC) fixture developed at the University of

Wyoming was used for the property testing [11]. The CLC method was chosen since sample $[90/0]_{8s}$ specimens tested at room temperature resulted in a higher ultimate compressive strength then obtained using other methods [7]. The other two methods evaluated were the ASTM standard using the IITRI fixture [12] and a method using the Short Block Compression fixture [13]. Additionally, there was increased simplicity of conducting the test using the CLC fixture.

The ultimate compressive strengths obtained from testing are presented in Table 2. The values are generally the average from 5 coupon specimens. Scatter in the data was as high as ±98. MPa for the unidirectional, $[0]_{32}$, laminates and as high as ±48. MPa for the other laminates tested. While using the CLC fixture in testing, observation on premature failures at elevated temperature were observed and through additional sample testing, were determined to be due to insufficient clamp-up pressure from the fixture. Additional clamp-up on the fixture was needed to prevent premature failure on the loaded ends of the specimen for the 177°C tests. An increase in torque to 6.8 N-m (from the recommended 2.8 N-m given in the user instructions) was found to be sufficient for failure to occur in the gage section. It was also found that using a torque too high, i.e. greater then 2.8 N-m for the -129°C tests, resulted in premature failure occurring in the gage section adjacent to the fixture.

Table 2. Experimental Data – Laminate Compressive Strength Properties

Test T (°C)	Lay-up				
	$[0]_{32}$ F_{xxC} (MPa)	$[90/0]_{8s}$ F_{xxC} (MPa)	$[+45/-45/0/90]_{4s}$ F_{xxC} (MPa)	$[+45/0/-45/90]_{4s}$ F_{xxC} (MPa)	$[+45/0_2,-45/0_2/+45/0_2/-45/0_2/+45/90_2/-45]_s$ F_{xxC} (MPa)
-129	1641.	993.	814.	793.	993.
21	1551.	869.	724.	641.	869.
177	1276.	655.	524.	476.	544.

The property data reveals that IM7/PETI5 laminate compressive strength decreases with increasing temperature. This is typical behavior for polymer matrix composite laminates where lamina compressive strength decreases with increasing temperature. For all lay-ups evaluated, the strength decrease in going from room temperature to the elevated temperature of 177°C was typically more severe than the strength increase in going to the cryogenic temperature of –129°C, although the change in temperature was nearly equivalent.

FINITE ELEMENT ANALYSIS

A finite element analysis study was conducted to determine the state of stress at failure of the $[90/0]_{8s}$ laminate and to aid in understanding both the mechanism for failure and the basis for the strength change with changing temperature. Each lamina is modeled as a continuum with orthotropic material properties. The laminate attributes that affect the state of stress were studied to establish the detail required to predict stress accurately in the laminates. The specific laminate attributes under investigation include: 1) the resin rich layer located between lamina in the laminate, 2) the residual thermal stresses that develop in a laminate due to the cure cycle, and 3) the temperature dependent stiffness and thermal expansion coefficients for the IM7/PETI5 lamina.

Due to in-plane symmetry in the $[90/0]_{8s}$ laminates, and the formidable computational size of the full three-dimensional problem, only this lay-up was chosen for investigation, where taking advantage of symmetry, only one-eight of the laminate is modeled. The gage section dimensions of the test specimens were chosen for the in-plane dimensions modeled. Two finite element geometry models of the $[90/0]_{8s}$ laminate were created, one without resin layers and one including resin layers between the laminae. The finite element model solid geometry including the resin-rich layers is shown in Figure 2. The model without the resin layers differed in that

a ply thickness of h = 0.014 cm is used, resulting in the same laminate half thickness of 0.224 cm. As approximated from the micrograph previously shown in Figure 1, for the model including the resin layer, the ply layer thickness, h, is 0.0127 cm, where the resin layer thickness is 0.1h. All ply layers have a thickness of h and resin layers have a thickness of 0.1h except the top ply has a thickness of h+0.05h and the one resin layer adjacent to the z=0 symmetry plane has a thickness of 0.05h. The total thickness modeled is 0.224 cm, which is half of the total laminate thickness of t = 0.447 cm. The three symmetry planes are z = 0, the through the thickness symmetry, and x = 0 and y = 0, the in-plane symmetry planes.

The finite element models consist of hexahedral solid elements with rectangular faces. A view in the x-y plane is displayed in Figure 3, where there are 20 uniformly spaced elements located in the x-direction and 34 elements in the y-direction. In the y-direction, 19 uniformly spaced elements are between y = 0 and y = 0.95W, and the remaining elements were graded with the maximum concentration located at the free edge, y = W. There are 112 element layers graded through the thickness of the model with resin layers which are not shown. The element layers are of increased density near z=0, where larger stress gradients were observed in preliminary analyses. A total of 76,160 elements are in the model including the resin layer.

The singularity that exists at the interface between lamina and the free edge in angle-ply laminates has been well documented where interlaminar stress solutions tend towards infinity. Convergence

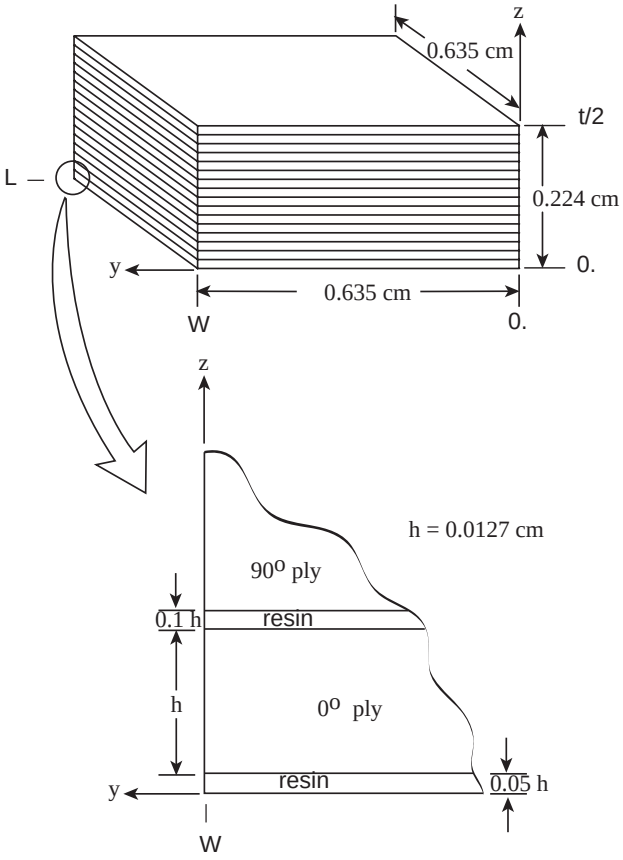

Figure 2. Finite element model solid geometry including resin-rich layer

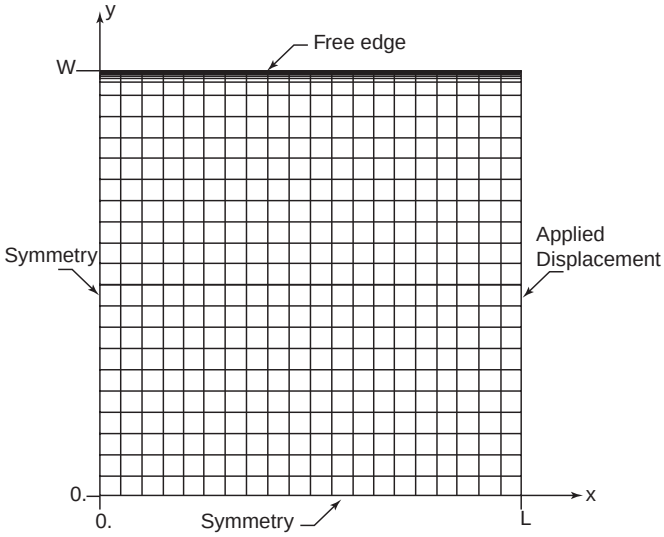

Figure 3. Finite element discretization in the x-y plane.

studies have shown the finite element solution is accurate except in a region involving the two elements closest to the singularity, and that this region without convergence can be made arbitrarily small by refining the finite element model [14,15]. Thus, the stresses to be presented here will all be at least two elements away from the free edge. With the two elements nearest the free edge being made extremely small, the solution two elements away, which is at a physical location 2. x 10^{-4} cm from the free edge boundary, is assumed to be a good approximate solution to the free edge stress [16]. The current mesh was concluded to be adequate since the results converged with results from a less refined mesh two elements away from the free edge of the less refined mesh[7]. The finite element analysis code NASTRAN is used to perform the structural analyses conducted herein [17].

Resin Layer Effect

To investigate the resin layer effect, the room temperature (21^{o}C) lamina engineering constants, as presented in Table 1 and Equations 1-5, are used as the properties in a linear static analysis of the composite laminate. For the $[90/0]_{8s}$ laminates, the average room temperature compressive strength of 869. MPa, as presented in Table 2, is used, along with the lamina moduli, E_{11c} and E_{22c}, to compute an equivalent applied displacement loading of d = - 0.007 cm for the analysis. The uniform displacement was applied on the surfaces at the end x = L on the finite element model as depicted in Figure 3.

Analysis results for the in-plane stresses, for the finite element model without the resin layer, closely replicate the Classical Lamination Theory (CLT) solution except for slight variations in a small region near the free edge, which is typically observed with computational analysis models. CLT predicted in-plane stresses of σ_x = -1590. MPa, σ_y = -47. MPa and σ_{xy} = 0. Analysis results of in-plane stresses from the finite element model including the resin layers were basically identical to the results obtained in the absence of the resin layers.

Analysis results for the interlaminar stresses are displayed in Figure 4. For σ_z, the location where peak tensile stresses occurred is displayed, since the tensile stress would tend to pull lamina apart and initiate failure. A maximum tensile σ_z = 49. MPa is predicted in the laminate without resin layers in the 0 degree ply along the z = 0 symmetry plane. For the model including resin layers, the maximum normal stress location was the same as obtained in the model without resin layers, however the maximum of σ_z = 60. MPa was over 20% greater when the resin layers were included in the model. A maximum σ_{yz} = -22. MPa occurred without the resin layers at the interface between the first 90 degree and 0 degree ply adjacent to the z = 0 symmetry plane. The maximum interlaminar shear stress, σ_{yz} = -44. MPa, occurred at the interface between the resin layer and 90 degree ply closest to the z=0 symmetry plane for the model with resin layers, a value twice as much as the maximum without resin layers. Since there is a great difference in interlaminar stresses between the models with and without resin layers, only the more detailed model including the resin layers will be utilized in the forthcoming analyses.

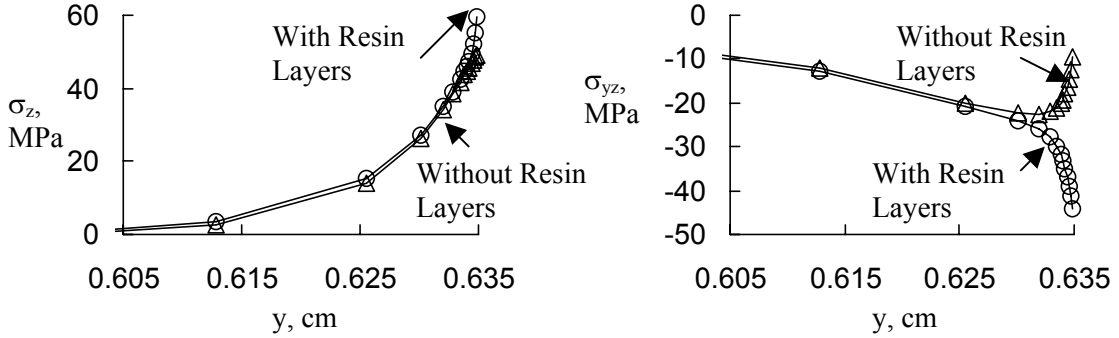

Figure 4. Interlaminar stresses in $[90/0]_{8s}$ laminate at x=0 , subject to applied displacement.

Thermal Residual Cure Stresses

The residual cure stresses in the composite laminate are investigated here using a linear analysis initiating from the SFT. Analyses were conducted for the three cases of the operating temperature being –129°C, 21°C, and 177°C. The properties at the relevant operating temperature as given in Table 1 are used. The interlaminar stresses were the most severe stresses in the laminate due to curing at all three operating temperatures of interest. Analysis results of the interlaminar stresses predicted at 21°C are plotted in Figure 5. A maximum tensile interlaminar normal stress of 48.8 MPa was predicted in the 90 degree ply at the interface of the first resin layer and 90 degree ply closest to z=0. A maximum interlaminar shear stress of 79.5 MPa was predicted in the resin layer at the interface of the first resin layer and 90 degree ply closest to z=0. Although the location of the maximum interlaminar stresses did not change at the different operating temperatures under consideration, the magnitudes predicted did and are presented in Table 3.

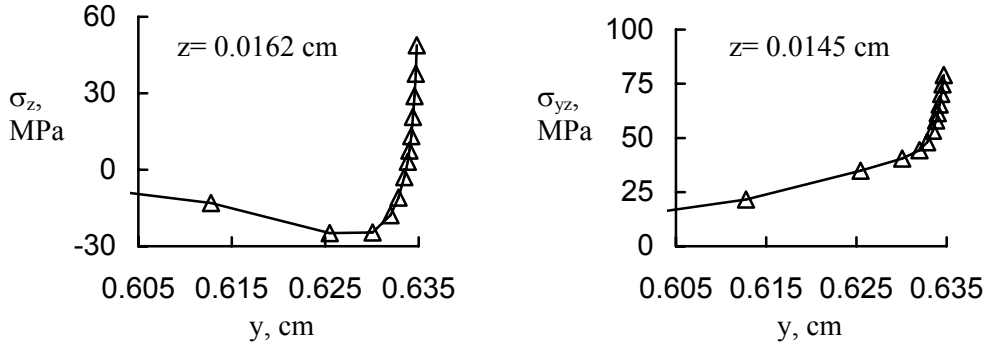

Figure 5. Interlaminar stresses in $[90/0]_{8s}$ laminate at 21°C due to curing only at x=0.

Temperature Dependent Material Properties

A nonlinear analysis of the composite laminate subject to the cure temperature changes is performed including temperature dependent material properties. A piecewise linear approximation of the material properties presented in Table 1 between the four temperatures given is incorporated in the finite element analysis. The temperature change loading was divided into ten increments with a convergence check made with a twenty increment division. The use of temperature dependent properties did not result in any change in the location of the maximum occurring interlaminar stresses and the difference in the magnitude in comparison to the analysis assuming constant properties was extremely insignificant at all operating temperatures. The maximum interlaminar stress results from the nonlinear analysis are presented in Table 3, in comparison to the linear analysis results.

Table 3. Comparison of Predicted Maximum Residual Cure Interlaminar Stresses

Temperature (°C)	Linear Analysis Constant Properties		Nonlinear Analysis Temperature-Dependent Properties	
	σ_z(MPa)	σ_{yz}(MPa)	σ_z(MPa)	σ_{yz}(MPa)
-129	53.	85.3	53.6	85.5
21	48.8	79.	49.4	79.1
177	10.5	16.8	10.5	16.8

Combined Loading

The analysis of residual cure stresses occurs from the stress free temperature of 238°C to the operating temperature. Then, at the operating temperature of interest, the applied displacement

loading occurs. The case of cure and the case of applied displacement loading at the operating temperature are analyzed independently where the states of stress are subsequently combined. The interlaminar stresses through the thickness of the laminate, two elements away from the free edge at x=0 are presented in Figure 6 at the operating temperature of 21°C. Shown in the figure in the upper two plots are the σ_z and σ_{yz} stresses obtained independently for the case of cure loading (dashed line) and applied displacement loading (solid line). The bottom two plots then show the combined solution of cure and applied displacement loading for σ_z and σ_{yz}. The stress distributions were very similar at the other operating temperatures analyzed, where the only variations were in the peak magnitudes, and hence were not also plotted. As can be observed from Figure 6 (which was the case for all except for σ_z at 177°C), the applied displacement load decreases the interlaminar residual stresses that are present in the laminate due to cure alone. At 177°C, the σ_z due to cure is smaller than σ_z due to the applied displacement, and consequently the net σ_z in the combined case is larger than σ_z from cure alone.

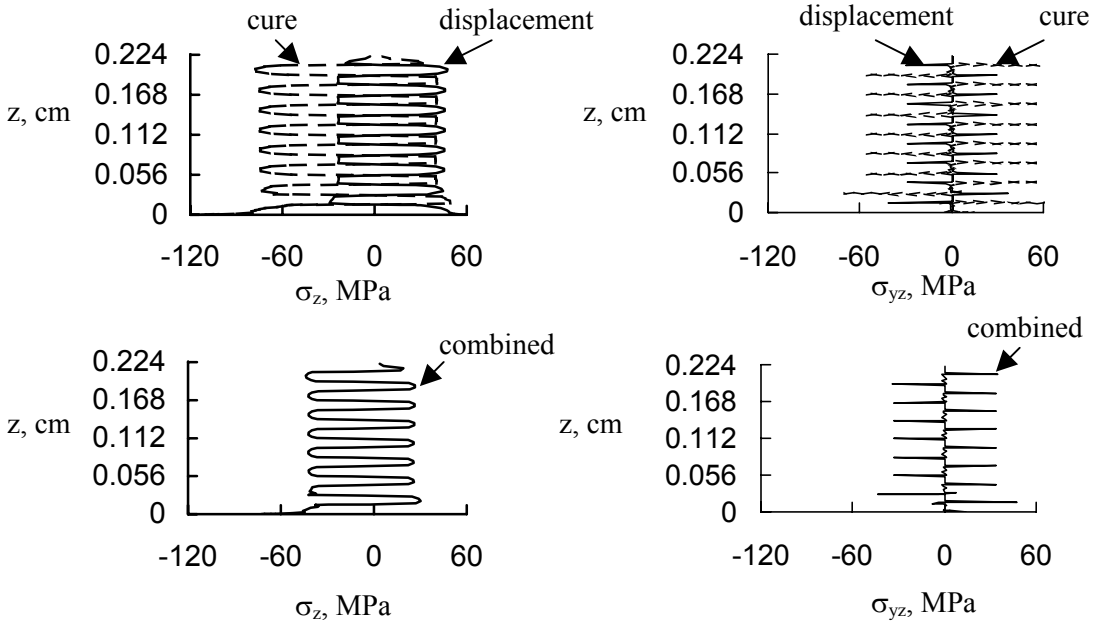

Figure 6. Interlaminar stresses through the thickness of the laminate at T = 21°C and x=0.

The only significant in-plane stress in the analysis model is σ_x in the 0 degree plies, where σ_{xy} was virtually zero and σ_y was much less than the y-direction strength, F_{22c}, in the 90 degree plies. Table 4 shows σ_x due to cure only, applied displacement only, and the combined case of cure and applied displacement loading. Although the presence of cure stresses intensifies the peak compressive in-plane stress, the magnitude of the in-plane cure stresses can be considered insignificant in comparison to the stresses due to the displacement loading. Unfortunately, the room temperature stress in the 0 degree plies for the combined loading, -1695. MPa, cannot be directly compared to the lamina compressive strength, F_{11c}, from Table 2, of 1551. MPa, because of the existence of resin layers in the unidirectional laminates used to determine F_{11c} for the lamina. The resin layers lead to cure stresses even in unidirectional laminates and their effect on lamina stress would need to be evaluated to compare with stresses in other angle-ply laminates.

Table 4. Maximum In-Plane Stress Predicted in the Laminate

Temperature (^{o}C)	σ_x (MPa)		
	Cure Only	Applied Displacement	Combined
-129	-110.2	-1591.6	-1701.8
21	-103.4	-1591.6	-1695.
177	-20.7	-1584.7	-1605.4

CONCLUDING REMARKS

The structural response of IM7/PETI5 laminates under large compressive loads has been studied for varying operating temperature. Laminate compression testing established the change in compressive strength at three operating temperatures of interest for several symmetric angle-ply laminate configurations.

Detailed finite element analyses of the IM7/PETI5 $[90/0]_{8s}$ composite laminate were conducted to study the laminate attributes necessary to predict stresses accurately. The significant laminate attributes that need to be included in the analysis of the laminate were determined to be: 1) the residual stresses due to cure and 2) the resin layer located between the lamina in the laminate. The analyses for this particular laminate establish that the temperature dependent material properties do not require a nonlinear analysis to provide an accurate stress solution. Modeling the laminate assuming the properties to be constant at the operating temperature of interest and conducting a more expeditious linear analysis is sufficient for predicting stresses accurately.

From the observation on the effect of an applied displacement load which decreases the interlaminar stresses present in the laminate due to cure alone, failure cannot be attributed to the interlaminar stresses in most of the cases studied for the $[90/0]_{8s}$ laminate when a compressive load is applied. However, experimental studies should be conducted to verify the magnitude of the cure stresses present in the laminates. One can conclude that the change in compressive strength of the $[90/0]_{8s}$ laminate due to a change in temperature is dominated by the change in lamina compressive strength. The secondary effect of changing in-plane residual stress in the 0-degree plies would then be to lessen the strength change for the laminate as compared to a theoretical laminate without residual cure stresses. Since resin layers were physically observed in the unidirectional laminates, the state of residual cures stress should also be evaluated and considered in the lamina strength characterization. Although interlaminar stresses do not appear to cause failure in a compression specimen, investigating the three-dimensional state of stress including thermal residual stresses was necessary to make this determination. Similarly, the three-dimensional state of stress in the other laminate configurations should be studied to determine the role of interlaminar stresses under the specific loading conditions of interest.

NOMENCLATURE

E	modulus of elasticity
G	shear modulus
h	ply thickness
L	length
T	temperature
T_g	glass transition temperature
W	width
t	laminate thickness
x,y,z	spatial coordinates
α	coefficient of thermal expansion
σ	stress

ν Poisson ratio

Subscript

1,2,3 spatial coordinate in lamina coordinate system
x,y,z spatial coordinate in global coordinate system
C compression
r resin layer
T tension

REFERENCES

1. Williams, Louis J.: HSCT Research Gathers Speed. *Aerospace America*, April 1995, pp. 32-37.
2. Sawyer, J.: Graphite-Composite Primary Structure for Reusable Launch Vehicles, 1996 AIAA Space Programs and Technologies Conference, September 24-26, Huntsville, AL, AIAA-96-4268, 1996.
3. Hou, T.H., Jensen, B.J., and Hergenrother, P.M.: Processing and Properties of IM7/PETI Composites, *Journal of Composite Materials*, vol. 30, no. 1, pp.109-122, January 1996.
4. Chamis, Christos C.: Lamination Residual Stresses in Multilayered Fiber Composites. *NASA TN D-6146*, February 1971.
5. Pagano, N.J. and Hahn, H.T.: Evaluation of Composite Curing Stresses. Composite Materials: Testing and Design (Fourth Conference), *ASTM STP 617*, American Society for Testing and Materials, 1977, pp. 317-329.
6. Chapin, C.M. and Joshi, S. P.: Variation of Residual Thermal Stresses in Graphite/Epoxy Laminates. *Composites: Proceedings of the 8th International Conference on Composite Materials*, Honolulu, HI, July 15-19, 1991, pp. 30-D-1 to 30-D-10.
7. Walker, S.P.: Thermal Effects on the Bearing Behavior of Composite Joints. PhD. Dissertation, University of Virginia, May 2001.
8. Chang, H.T.: Nonlinear Curing Analysis For Advanced Composite Materials. 35th International SAMPE Symposium, April 2-5, 1990, pp. 604-615.
9. Griffin, O.H.: Three-Dimensional Curing Stresses in Symmetric Cross-Ply Laminates with Temperature-Dependent Properties. *Journal of Composite Materials*, Vol. 17-September 1983, pp. 449-463.
10. Wu, C.M.L.: Nonlinear Thermal and Mechanical Analysis of Edge Effects in Angle-Ply Laminates. *Computers and Structures*, Vol. 35, No.6, 1990, pp. 705-717.
11. Adams, D.F. and Welsh, J.S.: The Wyoming Combined Loading Compression Test Method. *Journal of Composites Technology and Research*, JCTRER, Vol. 19, No. 3, 1997, pp. 123-133.
12. Annual Book of ASTM Standards, Sec.15, Vol. 15.03, D5961M-96, 1996, p. 310-323.
13. Masters, John E.: Compression Testing of Textile Composite Materials. NASA CR-198285, February 1996.
14. Raju, I.S. and Crews, J.H.: Interlaminar Stress Singularities at a Straight Free Edge in Composite Laminates. *Computers and Structures*, Vol. 14, No. 1-2, 1981, pp. 21-28.
15. Raju, I.S., Whitcomb, J.D., and Goree, J.G.: A New Look at Numerical Analysis of Free-Edge Stresses in Composite Laminates. NASA Technical Paper 1751, December 1980.
16. Reedy, E.D., Jr.: On Free-edge Interlaminar Stress Distributions. *Composites Science and Technology*, Vol. 34, 1989, pp. 259-266.
17. MSC/PATRAN/NASTRAN, Structural Analysis, Version 7, Vol. 1, The MacNeal-Schwendler Corperation, Los Angeles, CA, July, 1997.